NIPES

Journal of Energy Technology and Environment

Journal homepage: www.nipesjournals.org.ng

Buoyancy Reaction on Unsteady MHD Couette Flow in Free Convective Vertical Channels Due to Onset of Soret Effect

[1]B. Y. Isah and [2]F. Abdullah

[1]Department of Mathematics Usmanu Danfodiyo University, Sokoto P.M.B.2346, Sokoto State
[2]Department of Mathematics Waziri Ummaru Federal Polytechnic BirninKebbi, Kebbi State
[1]Corresponding author's E-Mail: isah.bala@udusok.edu.ng

Article Info

Article history:
Received 19 November 2020
Revised 25 November 2020
Accepted 16 December 2020
Available online 23 Dec. 2020

Keywords:
MHD, Soret effect, Buoyancy distribution effect, Heat Mass Transfer

https://doi.org/10.37933/nipes.e/2.2020.4

https://nipesjournals.org.ng

Abstract

A numerical investigation was carried out to study Soret effect on unsteady heat and mass transfer Couette flow in free convective vertical channels in the presence of buoyancy distribution effects due to ramped and isothermal temperature. The governing coupled non-linear partial differential equations of the flow were transformed into non-dimensional form using suitable dimensionless quantities. The non-linear time dependent momentum, energy and concentration equations under suitable initial and boundary conditions were solved using Finite Element Method (FEM). The expressions of velocity, temperature, concentration, skin friction, Nusselt number as well as Sherwood number have been obtained subject to isothermal and ramped temperature boundary conditions. Selected set of graphical results illustrating the effects of controlling parameters involved in the flow formations were discussed using line graphs. From the outcome of the results, it was revealed that increase of porosity parameter K, ratio of mass transfer parameter N, buoyancy effect term parameter r_t, Eckert number E_c and time parameter t enhances the velocity while reverse is the case with the with increase of Magnetic parameter M, Prandtl number P_r,Schmidt number S_c and time parameter t, Soret numberS_r and time parameter t. Similarly increase of porosity parameter K, ratio of mass transfer parameter N, buoyancy effect term parameter r_t, enhances the temperature profile and reverse is the case with the increase of, Prandtl number P_r. Also concentration profile get enhanced with the increase of Schmidt Sc and reverse is the case with increase of Soret number S_r.The skin friction at both y = 0 and y = 1 gets intensified with the increase Soret number and buoyancy parameter r_t for both ramped and isothermal temperature.

1. Introduction

The study of heat and mass transfer has indispensable applications in many wings of engineering. Due to its wide spectrum of engineering application, it provides mechanical engineers an idea of knowing the mechanisms of heat transfer involved in the operation of equipment, for example, boilers, condensers, air preheaters etc. In view of nuclear power planters, it gives them precise

information on heat transfer there by providing safe operation, which is an important factor in their design. Furthermore, combined heat mass and transfer also aids electrical engineers in avoiding material damage in electric motors, generators and transformers due to hot spots developed by improper heat transfer design and as well acquires knowledge of the efficient methods of heat dissipation from chips and semi-conductor devices so that they function within safe operating temperatures heat Nithiar [1]. Also, the study of heat and mass transfer of magneto fluids assist computer hardware engineers to know the cooling requirements of circuit boards, as the miniaturization of computing devices is advancing at a rapid rate. The simultaneous application of heat mass and transfer serves as the basis for understanding some of the important phenomena occurring in as food processing and polymer production.

An energy flux can be generated not only by temperature gradients but by composition gradients as well. Temperature gradients can generate mass fluxes and this is called thermal-diffusion (Soret) effects, while energy flux generated by composition gradients is called diffusion-thermo (Dufour) effects. Due to the importance of thermo-diffusion and diffusion-thermo effects for the fluids with very light molecular weight as well as medium molecular weight, many researchers have studied and reported results for these flows. Shankar and Rajashekar [2] analyzed the effects of thermo-diffusion chemical reaction and radiation absorption on an unsteady MHD convective heat and mass transfer flow of a semi-infinite vertical moving in a porous medium with heat source and suction and found that the increase in the Soret number leads to an enhancement in velocity. Similarly, Geethan [3], investigated thermo-diffusion and chemical reaction influence on combined heat and mass transfer MHD free convective boundary layer slip flow past an inclined plate in a porous medium in the presence of heat source and thermal radiation with constant heat and mass fluxes and revealed that, increase in Soret number rises the momentum and solutal boundary layer thickness. The effects diffusion thermo and thermo diffusion on unsteady MHD natural convection heat and mass transfer flow past an accelerated vertical porous plate in the presence of thermal radiation, variable temperature and also variable concentration were investigated by Chandra and Raju, [4] discovered that, the fluid velocity get enhanced with the increasing the value of Grashof number, modified Grashof number, porosity parameter, Soret number and Dufour number but a reverse trend was found in the case of magnetic parameter, Prandtl number. The temperature and concentration of the fluid get enhanced with the rise in Soret and Dufour number. Skin friction gets reduced with increase of both Soret and Dufour numbers and also Nusselt number decreases with increasing of Dufour number. Similarly, [5] studied the heat absorption, thermal-diffusion and diffusion- thermo effects on unsteady viscous incompressible MHD flow along semi-infinite inclined permeable moving plate with variable temperature and mass diffusion embedded in a porous medium and found that, an increase in the Prandtl decreases the temperature boundary layer while increase in the Dufour number, thermal radiation parameters and Eckert number enhances thermal boundary layer. Also an increase in the Soret number enhances the concentration boundary layer. The velocity rises with the increase in Dufour number, Soret number, Grashof number and solutal Grashof number. Similarly skin-friction and Nusselt number get intensified with the increase in Dufour number and Soret number while reverse is the case with Sherwood number. Bilal [6] analyzed the effect of mixed convection flow of an Oldroyd-B fluid is investigated in the presence of convective boundary condition and Soret and Dufour effects and found that effects of Soret number on temperature and concentration are reverse. Emmanuel, [7] investigated the effect of thermal diffusion and diffusion thermo on heat and mass transfer over a vertical porous surface with convective heat and mass transfer and found that combined effects of thermal diffusion and diffusion thermo and the other embedded

parameters can help control flow kinematics and enhances both the heat and mass transfer process. Also, Sasikumar and Govindarajan [8] studied the Soret effects on MHD Oscillatory flow with heat source in the presence of chemical reaction in an asymmetric wavy channel filled with porous medium is carried out and discovered that fluid velocity increases with increase in Soret number. Similarly, Gbadeyan, [9] presented free convective heat and mass transfer of an incompressible electrically conducting fluid in a finitely long vertical wavy channel, considering Soret, Dufour and chemical reaction effects in the presence of constant heat source or sink and concluded that mean velocity and temperature get reduced with increase in Dufour number and Soret number. Additionally, Idowu and Falodun [10] analyzed the effects of Soret and Dufour on MHD heat and mass transfer of a viscoelastic fluid pass over a semi-infinite vertical plate and concluded that fluid velocity and temperatures increase with increase in Dufour parameter. Also increase in Soret number leads to increase of fluid velocity and concentration

Reddy [11] studied an unsteady magnetohydromagnetic natural convection on the Couette flow of electrically conducting water at 4^0 C (Pr = 11.40) in a rotating system. The primary velocity, secondary velocity and temperature of water at 4^o C were obtained for both ramped temperature and isothermal plates and it was found that the primary velocity of the fluid increases with the increase of Gr and decreases with the increase of M^2, Ω^2 and Pr. The secondary velocity of the fluid increases with the increase of Gr and decreases with the increase of M^2 and Pr. Shagaiya and Daniel [12]) investigated the theoretical influence of buoyancy and thermal radiation on MHD flow over a stretching porous sheet. It was found that increase in buoyancy parameter intensifies the fluid velocity increase, the thermal boundary layer decreases. Increasing the thermal radiation parameter produces significant increases in the thermal conditions of the fluid temperature, which cause more fluid in the boundary layer due to buoyancy effect, causing the velocity in the fluid to increase. Shagaiya and Simon [13] analyzed influence of buoyancy and thermal radiation on MHD flow over a stretching porous sheet and found that when the buoyancy parameter increases, the fluid velocity increases and the thermal boundary layer decreases. Increasing the thermal radiation parameter produces significant increases in the thermal conditions of the fluid temperature, which cause more fluid in the boundary layer due to buoyancy effect, causing the velocity in the fluid to increase. Adamu and Bandari [14] studied the effect of thermal and solutal buoyancy parameters on the nanofluid flow, heat, and mass transfer characteristics due to a stretching sheet in the presence of a magnetic field and discovered that the axial velocity of the fluid increases with an increase of both thermal and solutal buoyancy parameter while thermal conductivity of the fluid decrease

The present numerical investigation used a promising and distinguished finite element analysis to address the effects of thermo-diffusion and buoyancy distribution reactions due to ramped and isothermal temperature as an extension to the pioneer work of Prabhakar [15]. It is novel to mention that the velocity temperature, concentration as well as shear stress have been obtained for both isothermal and continuous ramped temperature.

2. Formulation of the problem

Consider an unsteady free convective flow of an incompressible electrically conducting viscous dissipative fluid in finite vertical plates.

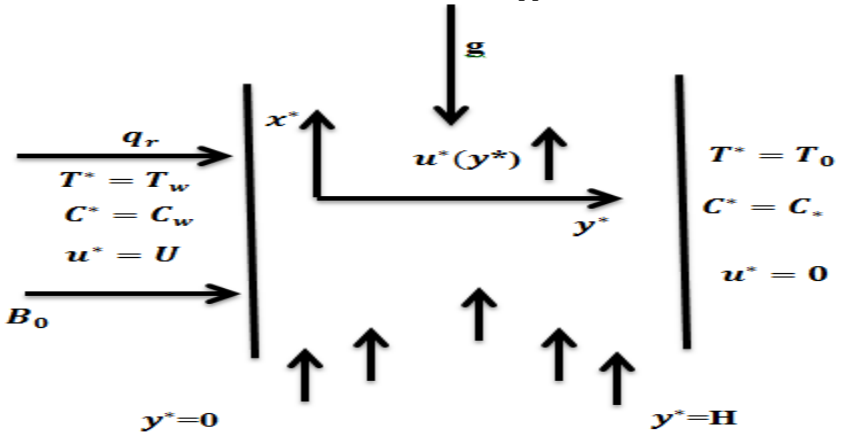

Figure 1: Geometry of the Problem

Let the x*-axis be chosen along the plate in the vertically upward direction and the y* axis is chosen normal to the plate. A uniform magnetic field of intensity B_0 is applied transversely to the plate. The induced magnetic field is neglected as the magnetic Reynolds number of the flow is taken to be very small. Initially, the temperature of the plate T^* and the fluid T_w^* are assumed to be the same. The concentration of species at the plate C_w^* and C_0^* are assumed to be the same. At time t*>0, the plate temperature is changed to T_w^*, which is then maintained constant, causing convection currents to flow near the plate and mass is supplied at a constant rate to the plate. Under these conditions the flow variables are functions of time t* and space (channel width) y* alone. By employing the Boussinesq approximation, the governing equations describing momentum, energy and mass transfer equations in the presence Soret effect, and other controlling parameters of the three problems take the following form:

Momentum equation

$$\frac{\partial u^*}{\partial t^*} = \frac{\partial^2 u^*}{\partial y^{*2}} + g\beta(T^* - T_w^*) - g\beta^{\bullet}(C^* - C_0) - \frac{\sigma\mu_e{}^2 H_0{}^2 u^*}{\rho} - \frac{\nu u^*}{K^*} \tag{1}$$

Heat Transfer equation

$$r C_p \frac{\partial T^*}{\partial t^*} = k\frac{\partial^2 T^*}{\partial y^{*2}} + Ec\left[\frac{\partial u^*}{\partial y^*}\right]^2 \tag{2}$$

Mass Transfer equation

$$\frac{\partial C^*}{\partial t^*} = D_M \frac{\partial^2 C^*}{\partial y^{*2}} + \frac{S_t \partial^2 T^*}{\alpha \partial y^{*2}} \tag{3}$$

The corresponding initial and boundary conditions are

Case I: Isothermal Temperature

$$\left.\begin{aligned} &t^* \le 0, u^* = 0, T^* = T_0 \ \ for\ \ all\ \ 0 \le y^* \le L \\ &t^* > 0 \begin{cases} u^* = u, T^* = T_w, C^* = C_w^* \ \ at\ \ y^* = 0 \\ u^* = 0, T^* = r_t^* T, C^* = C_w^* \ \ at\ \ y^* = L \end{cases} \end{aligned}\right\}$$

Case II: Continuous Ramped Temperature

$$\left.\begin{aligned} &t^* \le 0, u^* = 0, T^* = T_0 \ \ for\ \ all\ \ 0 \le y^* \le L \\ &t^* > 0 \begin{cases} u^* = u, T^* = T_0 + \dfrac{(T_w^* - T_0)t^*}{T_R}, C^* = C_w^* \ \ at\ \ y^* = 0 \\ u^* = 0, T^* = r_t^* T, C^* = C_w^* \ \ at\ \ y^* = L \end{cases} \end{aligned}\right\} \tag{4}$$

The non- dimensional quantities introduced in the above equations are defined as:

$$\left.\begin{array}{llll} U_0 = (vg\beta\Delta T)^{1/3}, & \mathrm{L}=\left(\frac{g\beta\Delta T}{\nu^2}\right)^{-1/3} & \mathrm{T}_R = \frac{(g\beta\Delta T)^{-2/3}}{\nu^{-1/3}} & \\ \Delta T = T_w^* - T_0^*, & \mathrm{t}=\frac{t^*}{T_R}, & \mathrm{y}=\frac{y^*}{L}, & \mathrm{r_t} = \frac{r_t^* - T_0}{T_w^* - T_0} \\ u = \frac{u^*}{U_0}, & \mathrm{K}=\frac{K^*}{\nu T_R}, & q=\frac{T^* - T_0}{T_w^* - T_0}, & f=\frac{C^* - C_0}{C_w^* - C_0} \\ \mathrm{Pr} = \frac{\mu C_P}{k}, & \mathrm{Sc}=\frac{\nu}{D_m}, & Ec = \frac{U_0^2}{C_P\Delta T}, & \mathrm{S_r}=\frac{S_t(T_w - T)_0}{\alpha(C_w - C_0)} \\ N = \frac{\beta'(C_w^* - C_\infty^*)}{\beta(T_w^* - T_0^*)}, & & M = \frac{\sigma m_0^2 H_0^2 T_R}{\rho} & \end{array}\right\} \quad \textbf{(5)}$$

Now on the substitution of Equations (5) into (1) - (4), the following governing equations in non-dimensional form are obtained:

$$\frac{\partial u}{\partial t} = \frac{\partial^2 u}{\partial y^2} + Gr\theta + N\phi - (M + \frac{1}{K})u \tag{6}$$

$$Pr\frac{\partial \theta}{\partial t} = \frac{\partial^2 \theta}{\partial y^2} + Ec\left(\frac{\partial u}{\partial y}\right)^2 \tag{7}$$

$$Sc\frac{\partial \phi}{\partial t} = \frac{\partial^2 \phi}{\partial y^2} + Sr\frac{\partial^2 \theta}{\partial y^2} \tag{8}$$

Case I: Isothermal Temperature

$$\left.\begin{array}{l} t \le 0,\ u = 0, \theta = 0, \phi = 0 \ \ for\ \ all\ \ y \\ For\ t \ge 0: \\ u = 1, \theta = 1, \phi = 1 \quad at\ \ y = 0 \\ u = 0, \theta = \mathrm{r_t}, \phi = 0 \quad at\ \ y = 1 \end{array}\right\}$$

Case II: Continuous Ramped Temperature

$$\left.\begin{array}{l} t \le 0,\ u = 0, \theta = 0, \phi = 0 \ \ for\ \ all\ \ y \\ For\ t \ge 0: \\ u = 1, \theta = t, \phi = 1 \quad at\ \ y = 0 \\ u = 0, \theta = \mathrm{r_t}, \phi = 0 \quad at\ \ y = 1 \end{array}\right\} \tag{9}$$

2.1 Method of the Solution

The method employed to solve the coupled non-linear system of partial differential equations was finite element method (Galerkin's approach) via the prescribe fundamental algorithms discuss in the work of Srinivasa [16].

Now subjecting Equation (6) via variational formulation to be solved under the boundary conditions (9) over a typical two nodded linear elements $y_i \le y \le y_j$ we get

$$\int_{y_i}^{y_j} \left\{ N^T \left[\frac{\partial^2 u}{\partial y^2} - \frac{\partial u}{\partial t} - u(M + \frac{1}{K}) + N\phi + \theta \right] \right\} dy = 0 \tag{10}$$

Equation (10) is reduce to

$$\int_{y_i}^{y_j} \left\{ N^T \left[\frac{\partial^2 u}{\partial y^2} - \frac{\partial u}{\partial t} - M_1 u + P \right] \right\} dy = 0 \tag{11}$$

$M_1 = M + \frac{1}{K}$ and $P = q + Nf$ Applying integration by part to Equation (11) yield;

$$[N^T \frac{\partial u}{\partial t}]_{y_i}^{y_j} - \int_{y_i}^{y_i} \frac{\partial N^T}{\partial y} \frac{\partial u}{\partial y} dy - \int_{y_i}^{y_i} N^T \frac{\partial u}{\partial t} dy - M_1 \int_{y_i}^{y_i} N^T u dy + P \int_{y_i}^{y_i} N^T dy = 0 \quad (12)$$

Dropping the first term of Equation (12)

$$\int_{y_i}^{y_i} \frac{\partial N^T}{\partial y} \frac{\partial u}{\partial y} dy + \int_{y_i}^{y_i} N^T \frac{\partial u}{\partial t} dy + M_1 \int_{y_i}^{y_i} N^T u dy - P \int_{y_i}^{y_i} N^T dy = 0 \quad (13)$$

Let $u^{(e)} = u_i N_i + u_j N_j \Rightarrow u^{(e)} = [N][u]^T$ be a linear piecewise approximation solution over the two nodal element $e,\ (y_i \le y \le y_j)$ where $u^{(e)} = [u_i\ u_j]$, $N = [N_i N_j]$ also u_i *and* u_j are the velocity component at the i^{th} and j^{th} nodes of the typical element $(e)\ \ (y_i \le y \le y_j)$ furthermore, N_i and N_j are basis (or shape) functions defined as follows:

$$N_i = \frac{y_j - y}{y_j - y_i},\quad N_j = \frac{y - y_i}{y_j - y_i}$$

Hence equation (13) take the form

$$\int_{y_i}^{y_i} \begin{bmatrix} N_i' N_i' & N_i' N_j' \\ N_i' N_j' & N_j' N_j' \end{bmatrix} \begin{bmatrix} u_i \\ u_j \end{bmatrix} dy + \int_{y_i}^{y_i} \begin{bmatrix} N_i N_i & N_i N_j \\ N_i N_j & N_j N_j \end{bmatrix} \begin{bmatrix} \dot{u}_i \\ \dot{u}_j \end{bmatrix} dy + M_1 \int_{y_i}^{y_i} \begin{bmatrix} N_i N_i & N_i N_j \\ N_i N_j & N_j N_j \end{bmatrix} \begin{bmatrix} u_i \\ u_j \end{bmatrix} dy - P \int_{y_i}^{y_i} \begin{bmatrix} N_i \\ N_j \end{bmatrix} dy = 0 \quad (14)$$

Simplifying equation (14) above we have;

$$\frac{1}{l}\begin{bmatrix} 1 & -1 \\ -1 & 1 \end{bmatrix}\begin{bmatrix} u_i \\ u_j \end{bmatrix} + \frac{l}{6}\begin{bmatrix} 2 & 1 \\ 1 & 2 \end{bmatrix}\begin{bmatrix} \dot{u}_i \\ \dot{u}_j \end{bmatrix} + \frac{M_1 l}{6}\begin{bmatrix} 2 & 1 \\ 1 & 2 \end{bmatrix}\begin{bmatrix} u_i \\ u_j \end{bmatrix} - \frac{lP}{2}\begin{bmatrix} 1 \\ 1 \end{bmatrix} = 0 \quad (15)$$

Where $l = y_j - y_i = h$ and prime and dot denotes differentiation with respect to y and t respectively. Assembling the Equations for the two consecutive elements $y_{i-1} \le y \le y_i$ and $y_i \le y \le y_{i+1}$ the following is obtained.

$$\frac{1}{l^2}\begin{bmatrix} 1 & -1 & 0 \\ -1 & 2 & -1 \\ 0 & -1 & 1 \end{bmatrix}\begin{bmatrix} u_{i-1} \\ u_i \\ u_{i+1} \end{bmatrix} + \frac{1}{6}\begin{bmatrix} 2 & 1 & 0 \\ 1 & 4 & 1 \\ 0 & 1 & 2 \end{bmatrix}\begin{bmatrix} \dot{u}_{i-1} \\ \dot{u}_i \\ \dot{u}_{i+1} \end{bmatrix} + \frac{M}{6}\begin{bmatrix} 2 & 1 & 0 \\ 1 & 4 & 1 \\ 0 & 1 & 2 \end{bmatrix}\begin{bmatrix} u_{i-1} \\ u_i \\ u_{i+1} \end{bmatrix} - \frac{P}{2}\begin{bmatrix} 1 \\ 2 \\ 1 \end{bmatrix} \quad (16)$$

Considering the row corresponding to the node i to zero with $l = h$, from Equation (16) the difference schemes reads

$$\frac{1}{h^2}(-u_{i-1} + 2u_i - u_{i+1}) + \frac{1}{6}(-\dot{u}_{i-1} + 4\dot{u}_i + \dot{u}_{i+1}) \frac{M_1}{6}(u_{i-1} + 4u_i + u_{i+1}) = P \quad (17)$$

Using the trapezoidal rule on (17), the following system of equations in Crank-Nicolson method are obtained as

$$A_1 u_{i-1}^{n+1} + A_2 u_i^{n+1} + A_3 u_{i+1}^{n+1} = A_4 u_{i-1}^{n} + A_5 u_i^{n} + A_6 u_{i+1}^{n} + P^* \tag{18}$$

Similarly, applying same trend employed to obtained (17), equations (7) and (8) be comes

$$B_1 q_{i-1}^{n+1} + B_2 q_i^{n+1} + B_3 q_{i+1}^{n+1} = B_4 q_{i-1}^{n} + B_5 q_i^{n} + B_6 q_{i+1}^{n} + Q^* \tag{19}$$

$$C_1 f_{i-1}^{n+1} + C_2 f_i^{n+1} + C_3 f_{i+1}^{n+1} = C_4 f_{i-1}^{n} + C_5 f_i^{n} + C_6 f_{i+1}^{n} + R^* \tag{20}$$

where

$$A_1 = 2 - 6r + rM_1 h^2, \quad A_2 = 8 + 12r + rM_1 h^2, \quad A_3 = 2 - 6r + rM_1 h^2$$

$$A_4 = 2 + 6r - rM_1 h^2, \quad A_5 = 8 - 12r - 4rrM_1 h^2, \quad A_6 = 2 + 6r - rM_1 h^2$$

$$B_1 = Pr - 3r, \quad B_2 = 4Pr + 6r, \quad B_3 = \Pr - 3r \quad B_4 = Pr + 3r,$$

$$B_5 = 4Pr - 6r, \quad B_6 = Pr + 3r$$

$$C_1 = Pr - 3r, \quad C_2 = 4Pr + 6r, \quad C_3 = \Pr - 3r$$

$$C_4 = Pr + 3r, \quad C_5 = 4Pr - 6r, \quad C_6 = Pr + 3r$$

$$P^* = 12rh^2(\theta_i^n + N\phi_i^n), \quad Q^* = 6r \Pr Ec\left[\frac{\partial u}{\partial y}\right]^2 \quad \text{and} \quad R^* = 6h^2 ScSr \frac{\partial^2 \theta}{\partial y^2}$$

Note that $r = \dfrac{k}{h^2}$ while h and k are the mesh size along y direction and time direction respectively. Index i refers to space and j refers to the time. In equations (14), (15) and (16), taking $i = 1(1)n$ and using the initials and boundary conditions (9), the following system of equations is obtained

$$A_i X_i = B_i \qquad i = 1(1)n$$

Where A_i matrices of are order n and X_i and B_i are column matrices having n components. The solution of the system of equation are obtained using Thomas algorithm for velocity, temperature and concentration. For various parameters the results are computed and presented graphically

The skin friction, Nusselt number and Sherwood number are important physical parameters for this type boundary layers flow. With known values of velocity, temperature and concentration fields, the skin-friction at the plate is given by non-dimensional form.

$$\tau = \left[\frac{\partial u}{\partial y}\right]_{y=0} \tag{21}$$

The rate of heat transfer coefficient can be obtained in the terms of Nusselt number in non-dimensional form, given as.

$$N_u = -\left[\frac{\partial \theta}{\partial y}\right]_{y=0} \tag{22}$$

The rate of mass transfer coefficient cab be obtained in terms of Sherwood number in non-dimensional form given by

$$S_b = -\left[\frac{\partial \phi}{\partial y}\right]_{y=0} \tag{23}$$

3. Results and Discussion

In order to address the reactions of underlying controlling parameters on flow region, finite element method was employed to solve the coupled, non-linear, dimensionless partial differential equations of the extended model. In the numerical computations arbitrary values were chosen for magnetic parameter (M), the Soret number (Sr), the Eckert number (Ec) the Schmidt number (Sc), the Ratio of mass transformation (N), the porosity parameter (K), the Buoyancy parameter (r_t) and Prandtl number (Pr) unless otherwise.

3.1 Velocity Profiles

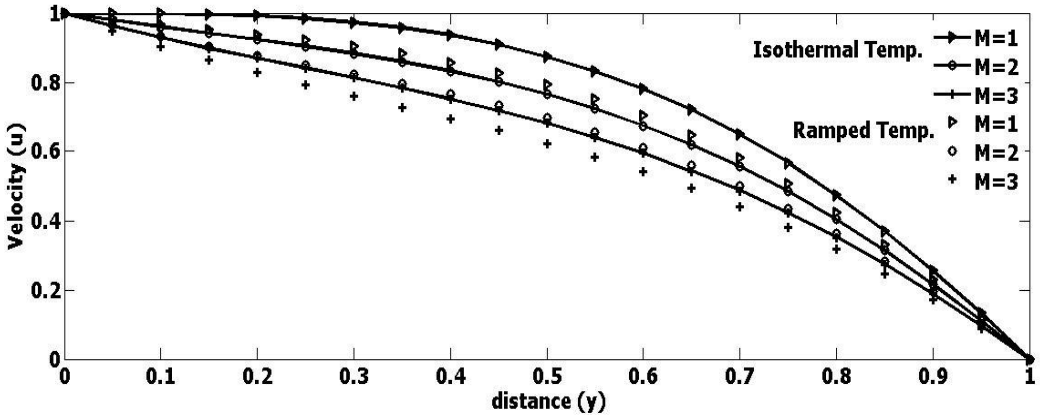

`Figure 2: Effect of M on velocity profile

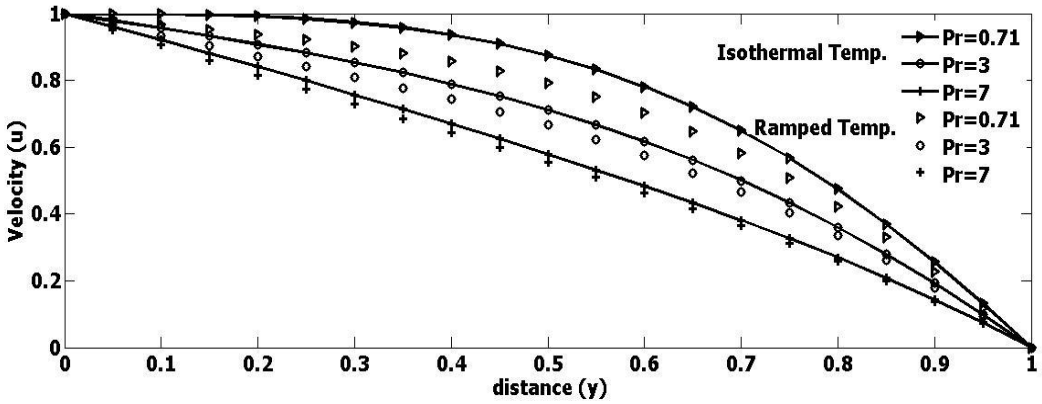

Figure 3: Effect Pr on velocity profile

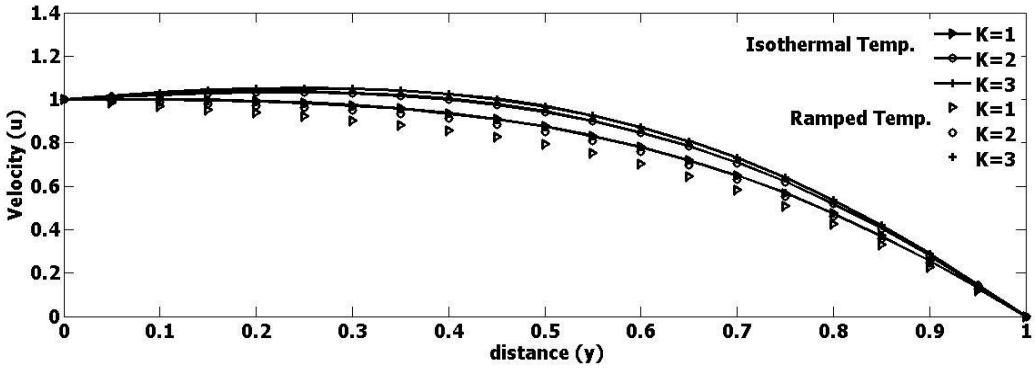

Figure 4: Effect of K on velocity profile

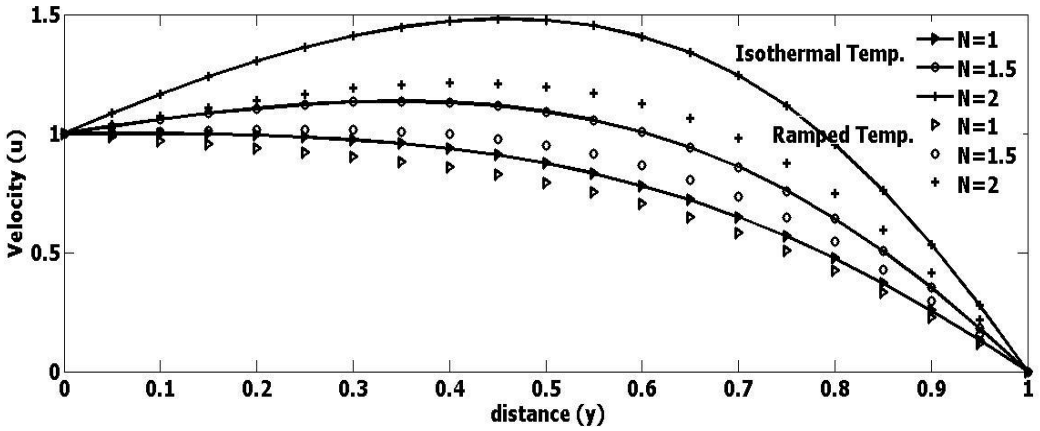

Figure 5: Effect of N on velocity profile

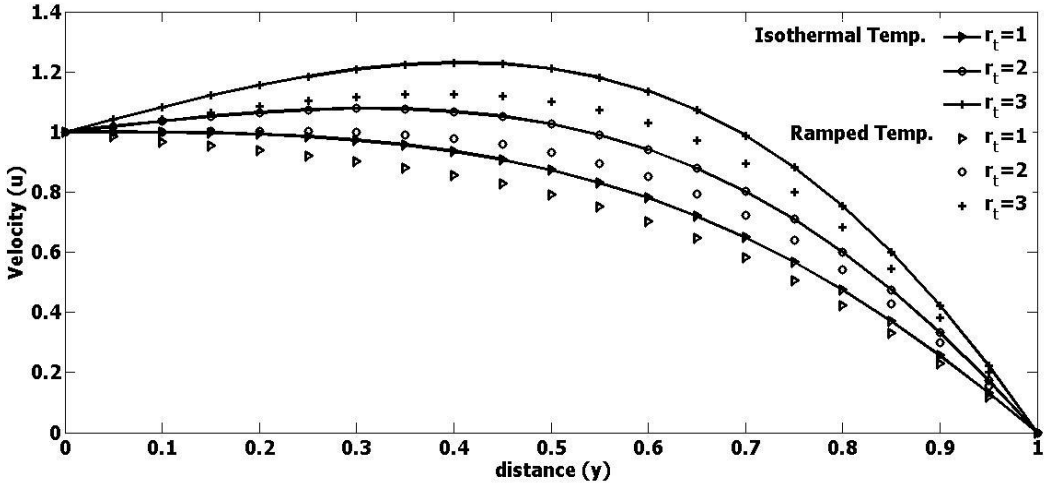

Figure 6: Effect r_t on velocity profile

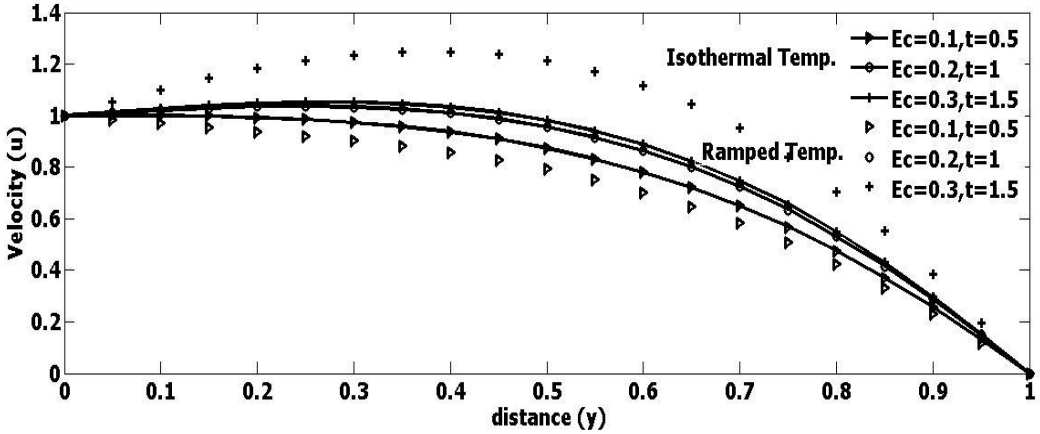

Figure 7: Effect Ec and t on velocity profile

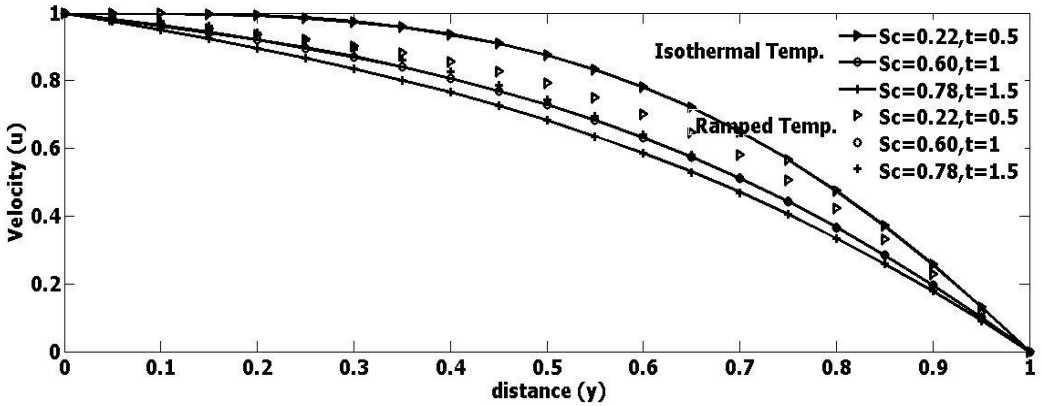

Figure 8: Effect Sc and t on velocity profile

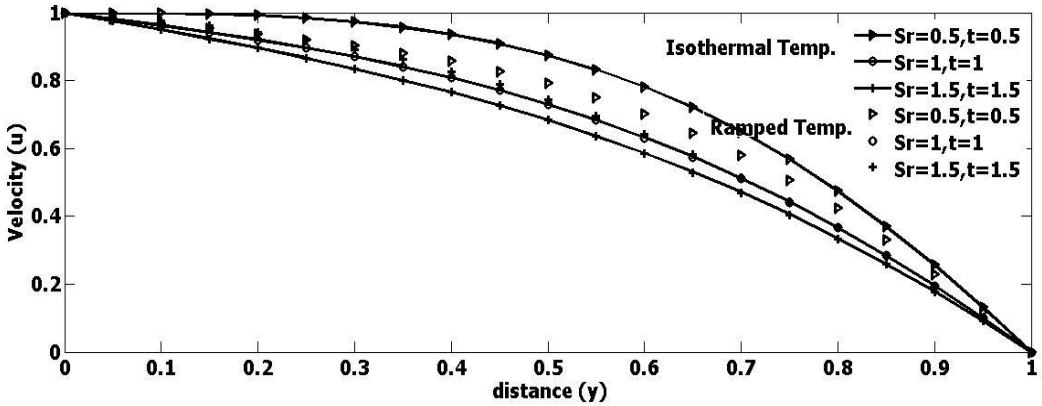

Figure 9: Effect Sr and t on velocity profile

Figure 2 gives the details about the control of magnetic parameter M on fluid velocity for both isothermal and ramped plate. From that Figure it is noticed that as magnetic parameter M rises the fluid velocity drop at all point of the flow field. This is true since magnetic parameter produce resistive force, which acts opposite direction to the fluid motion. Similarly Figure 3 displays the control Prandtl number Pr on fluid velocity for both isothermal and ramped plate. From that Figure it is revealed that as Prandtl number Pr increases the fluid velocity also fall off at all point of the flow field.

Figure 4 shows the effect control of porosity parameter K on fluid velocity for both isothermal and ramped plate and it is also observed that an increase porosity parameter K leads to rise in fluid velocity at all point of the flow. Similarly Figure 5 demonstrates the influence of the ratio of mass transfer parameter N on the fluid velocity for both isothermal and ramped plate. It is shown that increasing the values of the ratio of mass transfer parameter N for both isothermal and ramped plate enhances the fluid velocity with high impact due to ramped temperature. Likewise Figure 6 demonstrates the influence of buoyancy term r_t on the fluid velocity for both isothermal and ramped plate. It is also clearly observed that the fluid velocity significantly gets enlarged to for both isothermal and ramped plate by raising the values of buoyancy term.

Figure 7 displays the effect of Eckert number Ec and time t parameter on the fluid velocity for both isothermal and ramped plate. It is seen that increasing the values of Eckert number Ec and time

parameter t for both isothermal and ramped plate enhance the velocity. While opposite behavior is seen in Figure 8 and Figure 9 is the case of Schmidt number Sc and Soret number Sr respectively.

3.2 Temperature Profiles

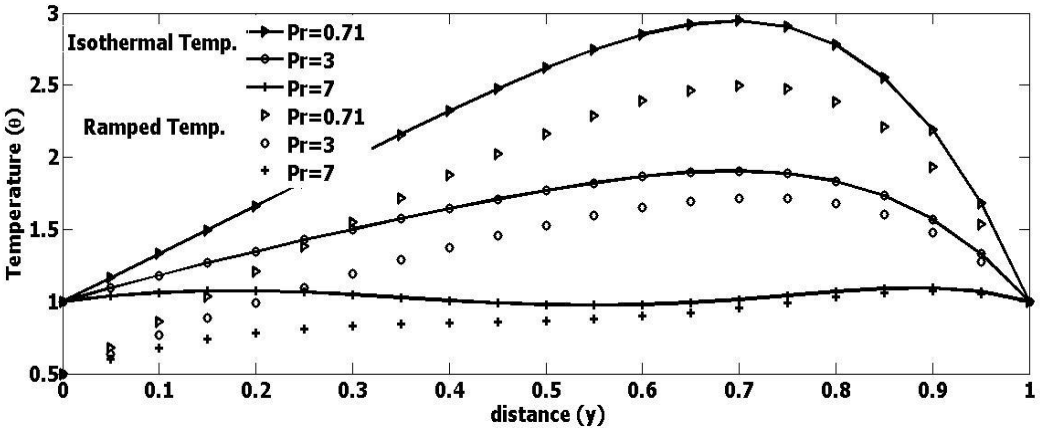

Figure 10: Effect Pr on temperature profile

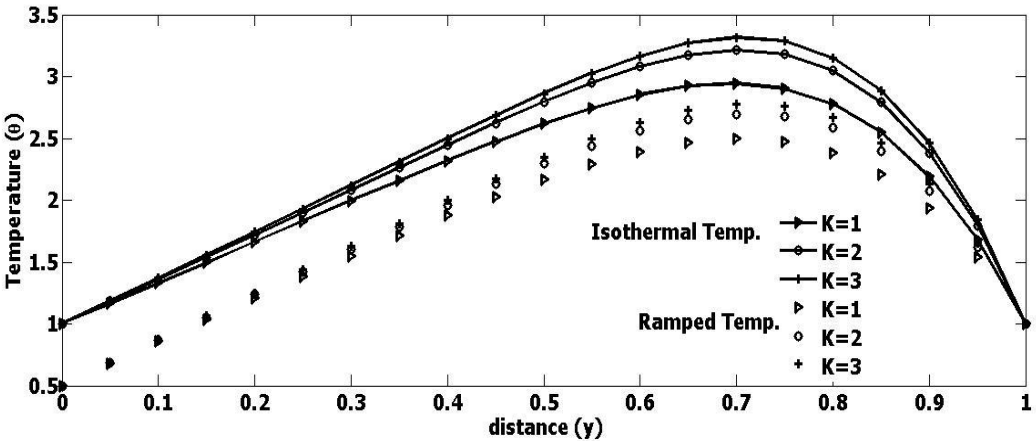

Figure 11: Effect of K on temperature profile

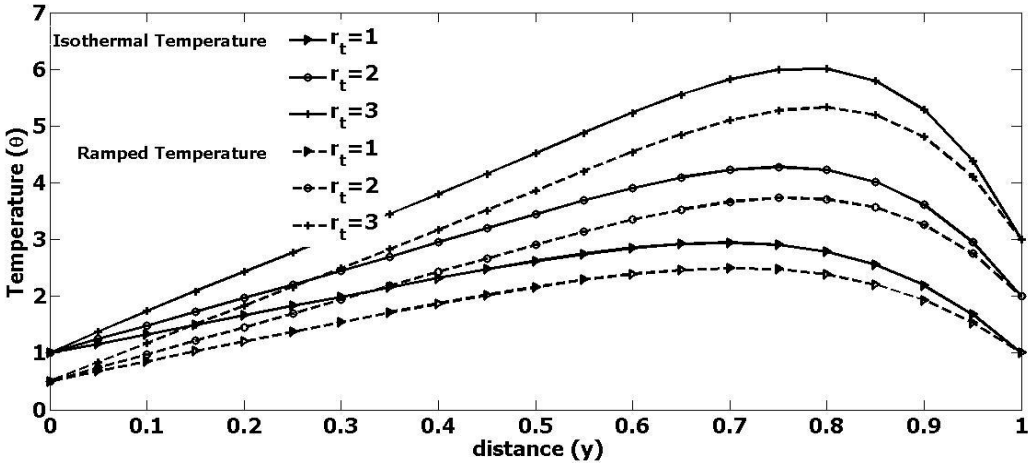

Figure 12: effect r_t on temperature profile

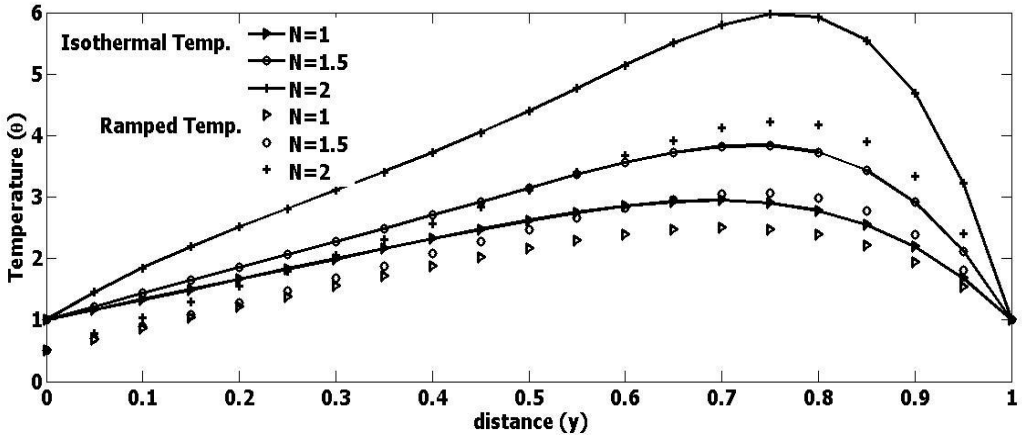

Figure 13: Effect N on temperature profile

Figure 10 depicts the influence of Prandtl number Pr on fluid temperature for both isothermal and ramped plate. It is revealed from that Figure the fluid temperature significantly gets diminished by increasing the values of Prandtl number which is usual trend that attribute to reduce thermal diffusivity at high values of Pr. While Figure 11 describes the influence of porosity parameter K on fluid temperature for both isothermal and ramped plate. It is revealed from that Figure that, the fluid temperature gets strengthen by increasing the values of porosity parameter K. Similarly Figure 12 depicts the effect of buoyancy parameter $r_t$on fluid temperature for both isothermal and ramped plate. It is clearly seen from that figure the fluid temperature gets intensified by increasing the values of buoyancy effect term r_t. Likewise Figure13 illustrates the effect of ratio of mass transfer parameter N on fluid temperature for both isothermal and ramped plate. It is also clearly seen from that figure the fluid temperature gets boosted by increasing the values of ratio of mass transfer parameter N for both isothermal and ramped plate.

3.3 Concentration Profiles

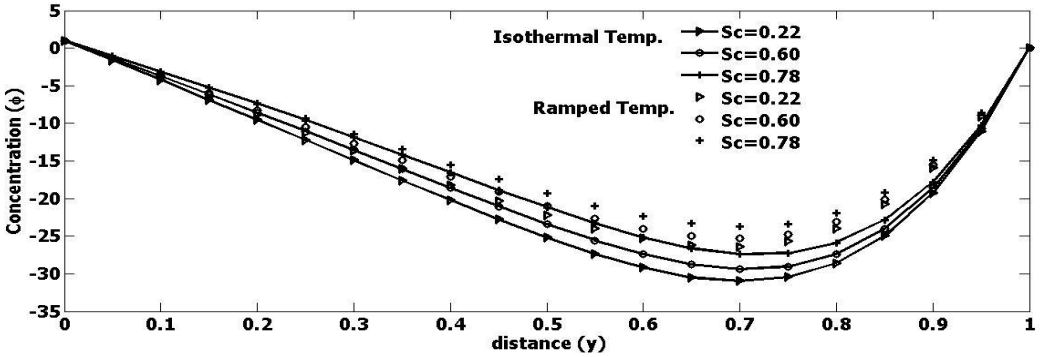

Figure 14: Effect Sc on concentration profile

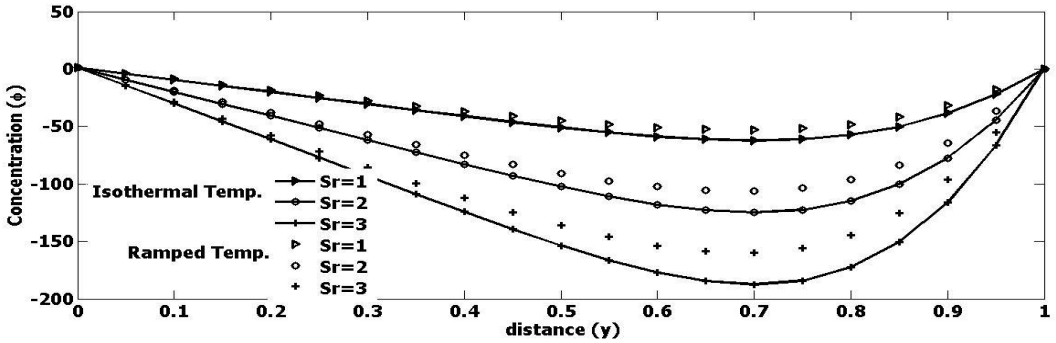

Figure 15: Effect Sr on concentration profile

Figure 14 displays the effect of Schmidt number Sc on the fluid concentration for both isothermal and ramped plate. It is seen that increasing the values of Schmidt number Sc raises fluid concentration. While opposite behavior is seen in Figure 15 in the case of Soret number Sr

3.4 Skin Friction Profile

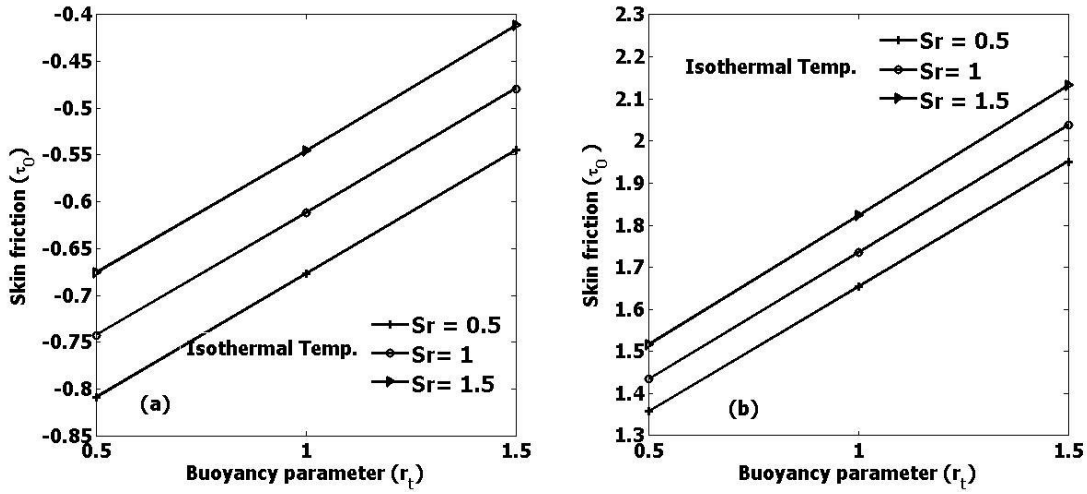

Figure 16: Effect of Sr and $\mathbf{r_t}$ on Skin friction due to the isothermal temperature

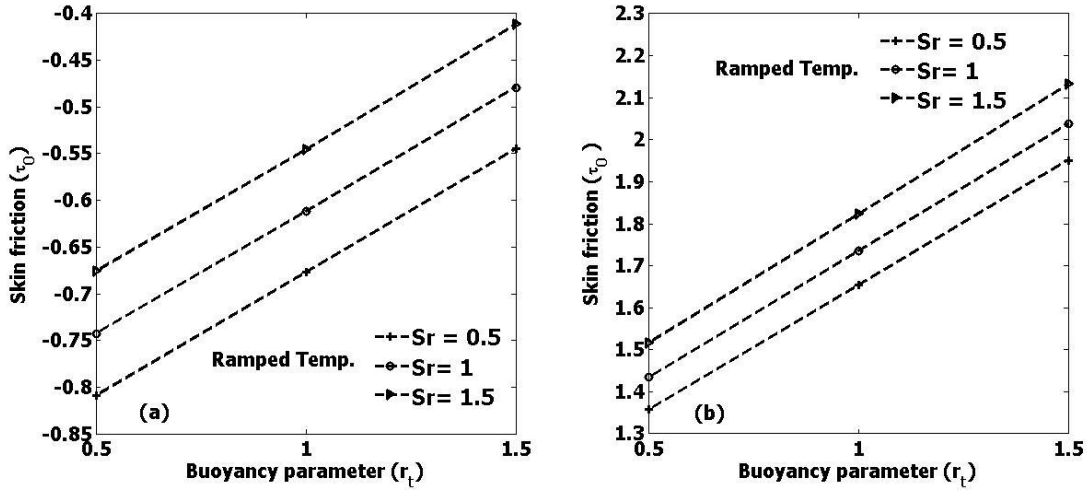

Figure 17: Effect of Sr and $\mathbf{r_t}$ on Skin friction due to the Ramped temperature

Figure 16 and 17 display the effect of Soret number and buoyancy parameter r_t on the fluid skin friction for both isothermal and ramped temperature at $y = 0$ and $y = 1$ respectively. It is clearly seen in both Figures that skin friction gets intensified with increase Soret number and buoyancy parameter r_t. However the values of skin friction in Figure 16 and 17(b) at $y = 1$ are raised higher in comparison with Figure 16 and 17(a) at $y = 0$.

3.5 Nusselt Number

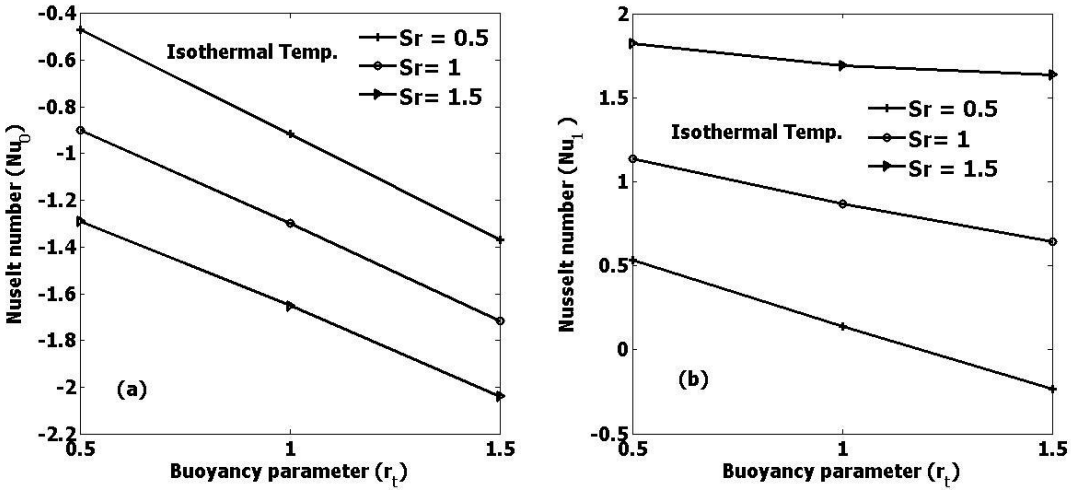

Figure 18: Effect Sr and r_t on Nusselt number due to isothermal temperature

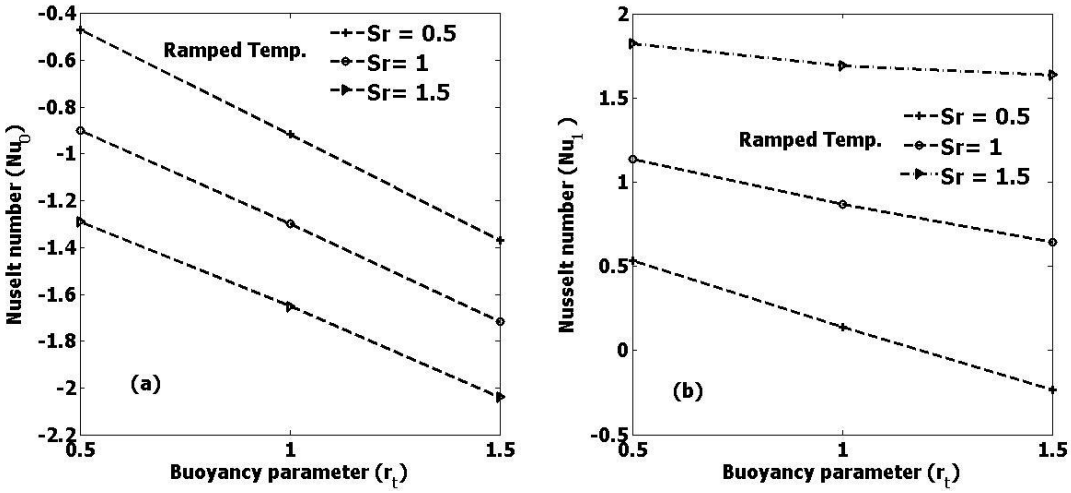

Figure 19: Effect Sr and r_t on Nusselt number due to ramped temperature

Figure 18 and 19 display the effect of Soret number and buoyancy parameter r_t on fluid Nusselt number for both isothermal and ramped temperature and it is clearly seen that the Nusselt number in Figures 18 and 19 (a) gets reduced by increasing both Soret number and buoyancy parameter r_t. While in figures 18 and 19 (b), fluid Nusselt number gets intensified with increase Soret number and gets diminished with increasing buoyancy parameter r_t.

3.6 Sherwood Number

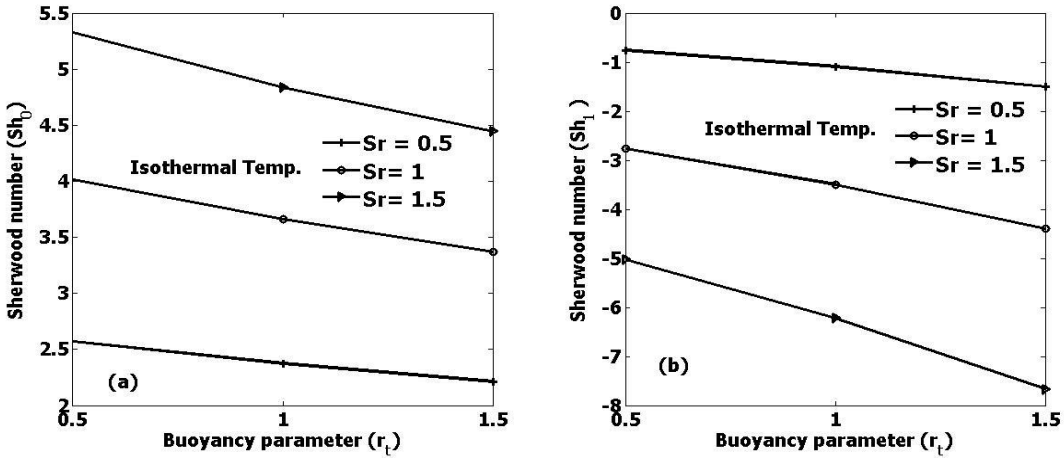

Figure 20: Effect Sr and r_t on Sherwood number due to the isothermal temp.

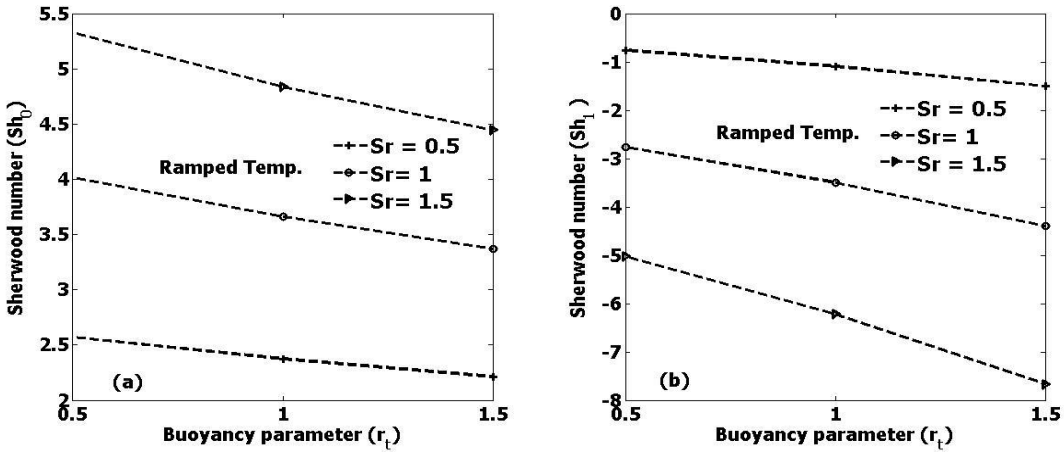

Figure 21: Effect Sr and r_t on Sherwood number due to the Isothermal temp.

Figure 20 and 21 display the effect of Soret number Sr and buoyancy parameter r_t on fluid Sherwood number for both isothermal and ramped temperature and it is clearly seen that the Sherwood number in Figures 20 and 21 (a), gets enhanced by increasing Soret number and gets reduced by increasing buoyancy parameter r_t. While in Figures 20 and 21 (b), fluid Sherwood number gets reduced with increase of Soret number buoyancy parameter r_t.

4. Conclusion

We studied the Soret effects on electrically conductive fluid of unsteady heat and mass transfer Couette in the presence of buoyancy distribution effects due to ramped and isothermal temperature. From the study, the following conclusions were drawn:

i. Increase of, porosity parameter K, ratio of mass transfer parameter N, buoyancy effect term parameter r_t, Eckert number Ec and time parameter t enhances the velocity while reverse is the case with the with increase of Magnetic parameter M, Prandtl number $\Pr$,Schmidt number Sc and time parameter t, Soret number Sr and time parameter t

ii. Similarly increase of Porosity parameter K, ratio of mass transfer parameter N, buoyancy effect term parameter r_t, enhances the temperature profile and reverse is the case with the increase of, Prandtl number Pr.

iii. There is enhancement of concentration profile with the increase of Schmidt Sc and reverse is the case with increase of Soret number Sr

iv. The skin friction at both y = 0 and y = 1 gets intensified with the increase Soret number and buoyancy parameter r_t for both ramped and isothermal temperature

v. Increase in Soret number and buoyancy parameter r_t diminishes Nusselt number at y = 0. Increase in Soret number also it enhances the Nusselt number at y=1, Increase buoyancy parameter diminishes the Nusselt number at y=1

vi. At y = 0, Increase in Soret number intensify Sherwood number, increase buoyancy parameter diminishes the Sherwood number. Similarly at y=1 Sherwood number get reduced with increase of Soret number buoyancy parameter

References

[1] Nithiarasu, R., Lewis, R. N. & Seetharmu, K. N (2016). *Fundamental of the Finite Element Method for Heat and Mass Transfer* (2nd Ed.). United Kingdom: John Wiley & Sons Ltd.

[2] Rajashekar, M. N & Shankar, B. G. (2016). Finite Element Method Application of Effects on an Unsteady MHD Convective Heat and Mass Transfer Flow In a Semi-infinite Vertical Moving in a Porous Medium with Heat Source and Suction, *Journal of Mathematics*, **12** (6), 55-64.

[3] Geethan, S. K., Kiran, R. K., Vinod, G. K. & Varma, S. V. K. (2016). Soret and Radiation Effects on MHD Free Convection Slip Flow over an Inclined Porous Plate with Heat and Mass Flux, *Advanced Science Engineering and Medicine*, **8** (3), 1-10.

[4] Chandra P. R., Raju M. C. & Raju, G. S. S. (2018). Magneto Hydrodynamic Convective Double Diffusive Laminar Boundary Layer Flow Past an Accelerated Vertical Plate, *International Journal of Engineering Research in Africa*, 20, 80-92.

[5] Reddy, S.S., Vijayabhaskar, C. & Mahendar, D. (2018). Unsteady MHD Flow over an Inclined Porous Plate Embedded in Porous Medium with Heat Absorption and Soret-Dufour Effects. *International Journal of Pure and Applied Mathematics*, **120** (6), 8021-8049.

[6] Bilal, M. A., Hayat, T., Alsaedi, A., Shehzad, A.S. (2016). Soret and Dufour effects on the mixed convection flow of an Oldroyd-B fluid with convective boundary conditions, *Results in Physics*, https://doi.org/10.1016/j.rinp.2016.11.009

[7] Emmanuel, M. A., Yakubu, I. S., Daniel, G. A. (2015). Analytical Solution of Dufour and Soret Effects on Hydromagnetic Flow Past a Vertical Plate Embedded in a Porous Medium, *Advances in Physics Theories and Applications*, **44**, 47 – 71.

[8] Sasikumar, J., and Govindarajan, A. (2019). Soret Effect on Chemically Radiating MHD Oscillatory Flow with Heat Source through Porous Medium in Asymmetric Wavy Channe, *National Conference on Mathematical Techniques and its Applications, https://doi:10.1088/1742-6596/1000/1/012034*

[9] Gbadeyan, J.A., Oyekunlec, T.L., Fasogbon, P.F., and. Abubakar, J.U. (2018). Soret and Dufour effects on heat and mass transfer in chemically reacting MHD flow through a wavy channel, *Journal of Taibah University For Science*, **5**(12) 631–651.

[10] Idowu, A.S., and Falodun, B.O. (2019). Soret–Dufour effects on MHD heat and mass transfer of Walter's-B viscoelastic fluid over a semi-infinite vertical plate: spectral relaxation analysis, *Journal of Taibah University for Science.* **13**(1) 49-62.

[11] Reddy, G. J., Raju, R. S., Rao, J. A. & Gorla, R. S. R. (2017). Unsteady MHD Heat Transfer in Couette Flow of Water at 4°C in a Rotating System with Ramped Temperature via Finite Element Method. *International Journal of Applied Mechanics and Engineering;* **22**(1), 145-161.

[12] Shagaiya, D. S. & Daniel, S. K. (2015). Effects of Buoyancy and Thermal Radiation on MHD Flow over a Stretching Porous Sheet using Homotopy Analysis Method. *Alexandria Engineering Journal;* **54**, 705-712.

[13] Shagaiya, Y. D. & Simon, K. D. (2015). Effects of buoyancy and thermal radiation on MHD flow over a stretching porous sheet using homotopy analysis method. *Alexandria Engineering Journal*, **54** (2015), 705-712

[14] Adamu, G. C., and Bandari, S. (2018). Buoyancy Effects on MHD Flow of a Nanofluid over a Stretching Sheet with Chemical Reaction. *International Journal of Innovative Research in Science, Engineering and Technology*, **7** (11), 2319-8753

[15] Prabhakar Reddy, B. (2016). Mass Transfer Effects on an Unsteady MHD Free Convective Flow of an Incompressible Viscous Dissipative Fluid Past an Infinite Vertical Porous Plate. *International Journa of Applied Mechanics and Engineering*, *https://doi:10.1515/ijame-2016-0009*

[16] Srinivasa Raju, R., Jithender Reddy, G., Anand, Rao, J. and Rashidi, M. M. (2016). Thermal Diffusion and Diffusion Thermo Effects on an Unsteady Heat and Mass Transfer Magnetohydrodynamic Natural Convection CouetteFlow Using FEM. *Journal of Computational Design and Engineering*, https://dx.doi.org/10.1016/j.jcde.2016.06.003